

SCIENTIFIC REPORTS



OPEN

Determination of pressure properties of superconducting systems based on characteristic ratios $2\Delta(0)/T_c$ and $\Delta C(T_c)/C_N(T_c)$

Mateusz Krzyzosiak¹, Ryszard Gonczarek², Adam Gonczarek³ & Lucjan Jacak²

A simplified analytical model of the effect of high pressure on the critical temperature and other thermodynamic properties of superconducting systems is developed using the general conformal transformation method and group-theoretical arguments. Relationships between the characteristic ratios $\mathcal{R}_1 \equiv 2\Delta(0)/T_c$ and $\mathcal{R}_2 \equiv \Delta C(T_c)/C_N(T_c)$ and the stability of the superconducting state is discussed. Including a single two-parameter fluctuation in the density of states, placed away from the Fermi level, stable solutions determined by \mathcal{R}_1 are found. It is shown that the critical temperature $T_c(p)$, as a function of high external pressure, can be predicted from experimental data, based on the values of the two characteristic ratios, the critical temperature, and a pressure coefficient measured at zero pressure. The model can be applied to *s*-wave low-temperature and high-temperature superconductors, as well as to some novel superconducting systems of the new generation. The problem of emergence of superconductivity under high pressure is explained as well. The discussion is illustrated by using experimental data for superconducting elements available in the literature. A criterion for compatibility of experimental data is formulated, allowing one to identify incompatible measurement data for superconducting systems for which the maximum or the minimum critical temperature is achieved under high pressure.

Recent discoveries of new classes of superconducting materials, with the most prominent example of iron-based superconductors, and ongoing development of superconductivity-based devices in the fields such as quantum information processing and fast digital circuits have kept superconductivity in the spotlight on the condensed matter physics stage. The accessibility of high-pressure experimental techniques has resulted in an advancement of characterization methods, providing a useful insight into the nature of superconductivity at high pressures in a wide class of materials. The amount of experimental data available has been also pushing forward research efforts on the theoretical front. In particular, many properties of novel superconducting systems under high external hydrostatic pressure have been recently studied by *ab-initio* numerical calculations^{1–11}. The results of these studies are usually in quite a good agreement of with the available experimental data. Being successful in providing quantitative characteristics of superconducting systems under high pressure, the *ab-initio* studies do not however provide much information about which of the system's parameters and to what extent affect these characteristics and material properties.

In refs^{12,13} we developed a simple analytical model of the effect of high pressure on the critical temperature and other thermodynamic properties of superconductors. The model allowed us to identify four general types of superconductors, based on the features of the T_c vs. pressure characteristics. The distinct behaviour of these four classes of superconductors can be studied with respect to the form of the density of states, which is determined within the so-called general conformal transformation method, taking into account fundamental properties and symmetry of the superconducting system.

¹University of Michigan-Shanghai Jiao Tong University Joint Institute, 800 Dongchuan Rd, Shanghai, 200240, China.

²Faculty of Fundamental Problems of Technology, Wrocław University of Technology, Wybrzeże Wyspiańskiego 27, 50-370, Wrocław, Poland. ³Faculty of Computer Science and Management, Wrocław University of Technology, Wybrzeże Wyspiańskiego 27, 50-370, Wrocław, Poland. Correspondence and requests for materials should be addressed to M.K. (email: m.krzyzosiak@sjtu.edu.cn)

In the present paper we illustrate the versatility of that model, by determining some properties of superconducting system based on experimental data. Within the model it is possible to study the characteristic ratio $\mathcal{R}_1 \equiv 2\Delta(0)/T_c$, that is a relation between the energy gap Δ at $T=0$ and the transition temperature T_c , and another characteristic ratio $\mathcal{R}_2 \equiv \Delta C(T_c)/C_N(T_c)$, where $\Delta C(T_c) = C_S(T_c) - C_N(T_c)$, defines the jump of the heat capacity between the superconducting and the normal phase at the transition temperature. The fundamental thermodynamic quantities defining the ratios \mathcal{R}_1 and \mathcal{R}_2 , and hence the ratios themselves, can be measured using experimental techniques and are widely reported in the literature^{5,14–23}. Therefore experimental results can be easily compared against theoretical predictions, in a way that is presented in this paper.

Because of intrinsic uncertainty of experimental methods, the experimentally found values of material parameters have limited accuracy, usually of the order of a few percent. Moreover, different experimental techniques may provide different estimates for the same parameter. However, these fluctuations are again usually of the order of a few percent. Therefore, the numerical results given below, although derived within the specified precision, should be treated as estimates and may be subject to minor changes, depending on the precision of the experimental data available.

Method

Numerous properties of various classes of superconductors, including *s*-wave low-temperature and high-temperature superconductors, as well as superconducting systems on the new generation, can be studied by within a simple analytical model, based on the general conformal transformation method and justified using group-theoretical arguments^{13,24–32}.

Conformal transformation method. The general conformal transformation method allows us to transfer any model of a superconducting system formulated in the original reciprocal (momentum) space to a mathematically fully equivalent model in an isotropic reciprocal space. The fact that the space becomes isotropic, does not mean that the method simply neglects some degrees of freedom: They are instead encoded in an involved function of two (or three) variables, that in the conformal transformation method replaces the usual electronic density of states. All properties of the system included originally in the dispersion relation, are transferred to this new function – a scalar field of the density of states.

More formally, applying the conformal transformation with elements of the group theory, we arrive at a mathematically equivalent description in an isotropic reciprocal space. The symmetry of the superconducting energy gap follows then from a requirement of choosing an appropriate subspace of irreducible representations, yielding a scalar field of the density of states. This field, for a trivial representation — corresponding to the *s*-wave symmetry — reduces to the standard electronic density of states. In other, more complicated scenarios, for $T = T_c$ (and $\Delta = 0$), the scalar density of states is averaged with the spherical harmonics (for 3D systems) or the Fourier harmonics (in the 2D case). This procedure, eventually, also yields a density-of-states-type function. Consequently, the pairing potential, which in general has a spin-antisymmetric or a spin-symmetric structure, becomes expressed in terms of a double series of the spherical harmonics (or the Fourier harmonics) indexed by the number l for 3D (or 2D) systems. For the spin-antisymmetric part, only the harmonics with even values of l are included, whereas for the spin-symmetric part — only those with odd values. Finally, it is enough to take $l = 0$ and assume the pairing interaction amplitude g to be just a constant function. Then the scalar field of the density of states reduces to the density of states.

The density of states and the averaged density-of-states-type function are quite complicated functions, but in general we expect them to feature some fluctuations. The fluctuations can be either positive (peaks) or negative (valleys). The case that we have discussed in our previous paper³³ and also discuss in the present work, is that of a density of states featuring a single two-parameter Dirac- δ type fluctuation, placed away from the Fermi level. This fluctuation (a peak) is imposed onto an otherwise constant-value density of states characteristic to the BCS model. This simplification makes an arbitrary model of a superconductor to eventually correspond to a model of a *s*-wave superconductor. As we argue above, it is a natural consequence of the used mathematical formalism and not an *a priori* assumption (which would have been incorrect).

Pressure effects. The method we use to include the hydrostatic pressure in our model is presented and discussed in detail in ref.³³. Therefore, in this subsection we just recall its main idea: The approach starts out from a set of two equations for a pressure-free system ($p = 0$). One of these equations is the superconducting gap equation, derived within the Green function formalism in the mean-field approximation. Another self-consistent equation for the carrier concentration completes the set and brings about equations describing the thermodynamic properties of the superconductor taking into account external pressure.

External pressure imposed on a superconducting sample leads to a stable configuration under new conditions. In particular, the new equilibrium yields a modified dispersion relation for charge carriers, parametrized now by the external pressure. More specifically, high pressure, applied to a superconducting sample, supplies an extra amount of energy to each unit cell. The amount of that additional energy is absorbed by unit cell atoms, and hence a new equilibrium state is reached with the dispersion relation, parametrized also by the pressure p .

In the following sections we assess the impact of high pressure on the critical temperature, based on experimental data for the characteristic ratios \mathcal{R}_1 and \mathcal{R}_2 for various superconductors, and using results obtained within the above outlined conformal transformation method^{13,24–33}. In particular, we discuss the relationship between the values of the characteristic ratios \mathcal{R}_1 , \mathcal{R}_2 and the stability of the superconducting state. We find stable solutions for superconducting systems determined by these characteristic ratios and some additional restrictions.

In order to describe pressure effects within the conformal transformation method, we assume that the peak in the density of states may be located either above or below the Fermi level, at the point $X_0 = 2T_c x_0$. The dimensionless density of states itself is taken in the form $\mathcal{N}(\xi) = 1 + 2\chi\delta(x - x_0)$, where the parameter χ is the height of

the local fluctuation, that can be either positive (corresponding to a peak) as well as negative (a valley). As we show in the paper, within our model we are able to reproduce experimentally observed T_c vs pressure dependence for various superconducting materials. This suggests that it is the fluctuations (peaks/valleys) in the DOS, emerging in the conformal transformation method, that imply the type of the T_c vs pressure response.

Critical Temperature and Characteristic Ratios for a Pressure-Free System

Critical temperature. Within the model featuring a single fluctuation in the density of states function of form $2\chi\delta(x - x_0)$, the critical temperature $T = T_c(\chi, x_0)$, when $\Delta = 0$, can be found as³³

$$T_c(\chi, x_0) = T_c(0, 0) \exp\left[\chi \frac{\tanh x_0}{x_0}\right], \tag{1}$$

where $T_c(0, 0)$ is the critical temperature in the standard BCS-type model, with

$$T_c(0, 0) = \frac{\xi_p}{k_B} \exp\left[-\frac{1}{\nu_0 g}\right]. \tag{2}$$

The so-called cut-off parameter ξ_p in formula (2) is determined individually for each superconducting system and depends on details of the pairing mechanism¹³. For systems with an electron-phonon pairing potential the cut-off parameter corresponds to the Debye energy $k_B T_D$, where k_B is the Boltzmann's constant and T_D denotes the Debye temperature. The dimensionless amplitude of the pairing interaction is $\nu_0 g$, with ν_0 being the density of states of the BCS type.

Ratios \mathcal{R}_1 and \mathcal{R}_2 . The characteristic ratio $\mathcal{R}_1(\chi, x_0) = 2\Delta(0, \chi, x_0)/T_c(\chi, x_0)$ as a function χ and x_0 is found from the following equation³³

$$\mathcal{R}_1(\chi, x_0) = \mathcal{R}_1^* \exp\left\{\chi \left[\frac{4}{\sqrt{(4x_0)^2 + \mathcal{R}_1^2(\chi, x_0)}} - \frac{\tanh x_0}{x_0} \right]\right\}, \tag{3}$$

where $\mathcal{R}_1^* = 2\pi e^{-C}$ is the characteristic ratio \mathcal{R}_1 for the BCS case ($\chi = 0$), and C denotes the Euler constant. The ratio $\mathcal{R}_1(\chi, x_0)$ is found numerically, assuming that $2 \leq \mathcal{R}_1(\chi, x_0) \leq 6$.

The other characteristic ratio $\mathcal{R}_2 \equiv \Delta C(T_c)/C_N(T_c)$, where $\Delta C(T_c) = C_S(T_c) - C_N(T_c)$, quantifying the jump of the heat capacity between the superconducting and the normal phase at the transition temperature, is also a function of χ and x_0 . Referring again to results presented in ref.³³, the value of the ratio can be found as

$$\mathcal{R}_2(\chi, x_0) = \frac{6 \exp\left(\chi \frac{\tanh x_0}{x_0}\right)}{\pi^2 a \left[1 + \frac{\chi}{3a} \varphi(x_0)\right]}, \tag{4}$$

where $a = 7\zeta(3)/2\pi^2$ and $\varphi(x) = \frac{3}{2x^3}(\tanh x - x \cosh^{-2} x)$, with $\zeta(n)$ denoting the Riemann- ζ function. Note that $\zeta(3) = 1.202056 \dots$, and $\varphi(x) \leq 1$ is an even and positive function of the real variable x . Moreover, $\varphi(0) = 1$ and it quickly approaches 0 as $|x|$ increases from 0 to ∞ .

From Eq. (3), the parameter χ can be found in terms of \mathcal{R}_1 and x_0 , and substituted into Eq. (4). Eventually, the ratio \mathcal{R}_2 as a function of \mathcal{R}_1 and x_0 is found as

$$\mathcal{R}_2 = \frac{6}{\pi^2 a} \exp\left[\frac{\tanh x_0}{x_0} \frac{\sqrt{(4x_0)^2 + \mathcal{R}_1^2} \ln(\mathcal{R}_1/\mathcal{R}_1^*)}{4 - \frac{\tanh x_0}{x_0} \sqrt{(4x_0)^2 + \mathcal{R}_1^2}} \right] \times \left[1 + \frac{\varphi(x_0) \sqrt{(4x_0)^2 + \mathcal{R}_1^2} \ln(\mathcal{R}_1/\mathcal{R}_1^*)}{3a \left[4 - \frac{\tanh x_0}{x_0} \sqrt{(4x_0)^2 + \mathcal{R}_1^2}\right]} \right]^{-1}, \tag{5}$$

where $\mathcal{R}_1^* = 3.527756 \dots$, $a = 0.426278 \dots$, $\frac{6}{\pi^2 a} = 1.426104 \dots$. The formula (5), in the specific case $x_0 = 0$, has proved to provide a good fit to experimental data for some low-temperature superconducting materials²⁴. Note that the right-hand sides of expressions (1), (3), (4), and (5) are all even functions of x_0 . This allows us to use Eq. (5) to derive just $|x_0|$, when \mathcal{R}_1 and \mathcal{R}_2 are known from experimental data.

We supplement the set of equations for a pressure-free system with a formula for the free energy difference ΔF . The formula, derived for the sub-critical temperature range, *i.e.* for $T \lesssim T_c(\chi)$, in the first order of the perturbation method, has the form³³

$$\Delta F(T, \chi, x_0) = -\frac{\nu_0 T_c^2(\chi, x_0)}{a \left[1 + \frac{\chi}{3a} \varphi(x_0)\right]} \left[1 - \frac{T}{T_c(\chi, x_0)}\right]^2. \tag{6}$$

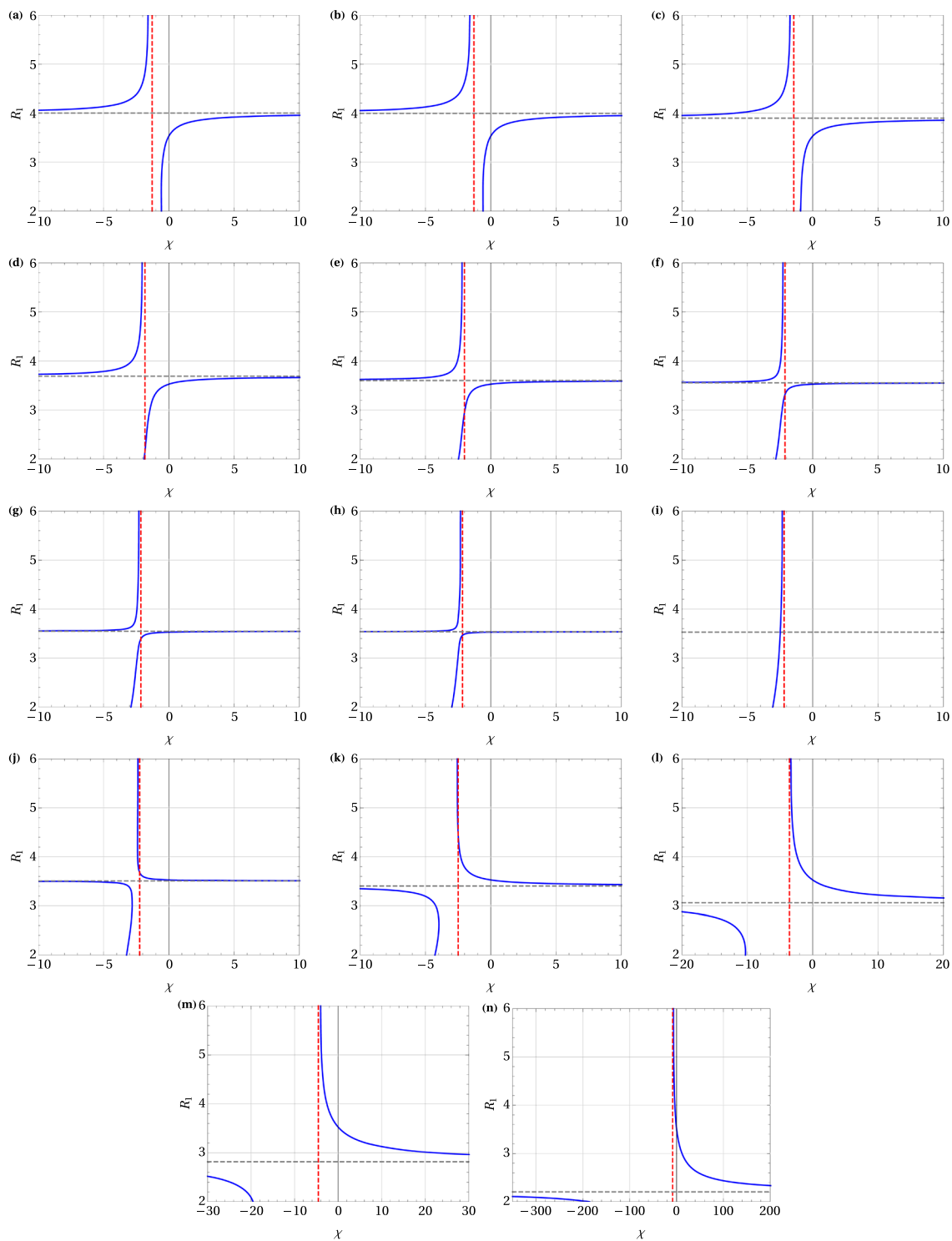


Figure 1. Ratio \mathcal{R}_1 as a function of the parameter χ for selected values of x_0 : (a) 0, (b) ± 0.1 , (c) ± 0.4 , (d) ± 0.7 , (e) ± 0.8 , (f) ± 0.85 , (g) ± 0.86 , (h) ± 0.87 , (i) ± 0.8791 , (j) ± 0.9 , (k) ± 1 , (l) ± 1.3 , (m) ± 1.5 , (n) ± 2 .

Note that a system can be in the superconducting state only if $\Delta F(T, \chi, x_0) < 0$, and it occurs if $1 + \frac{\chi}{3a} \varphi(x_0) > 0$.

Forms of the characteristic ratio $\mathcal{R}_1(\chi, x_0)$. In this subsection we discuss solutions to Eq. (3) for several selected values of x_0 . We find $\mathcal{R}_1(\chi, x_0)$, which is an even function of x_0 , numerically in dependence on χ . The solutions, shown in Fig. 1 and discussed in detail later in this section, have a common feature: there are two separate curves in each graph, with a horizontal asymptote $\mathcal{R}_1 = \mathcal{R}_A(x_0)$, where

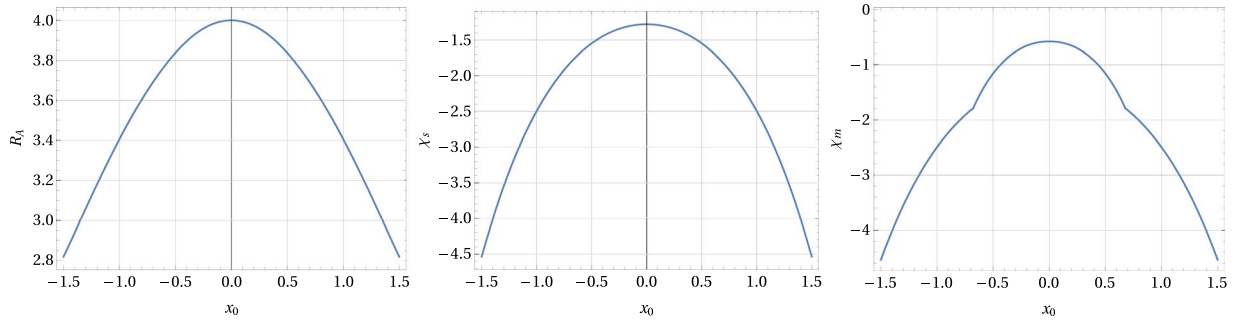


Figure 2. The values of \mathcal{R}_A (defining horizontal asymptotes), the vertical cut-off line χ_s (delineating unstable regions), and the minimum value of $\chi \equiv \chi_m$ for which superconducting state can be realized, are shown here as functions of x_0 .

$$\mathcal{R}_A(x) = \frac{4x}{\sinh x}, \tag{7}$$

and $\mathcal{R}_A(x_0) = \mathcal{R}_1^*$ for $x_0 \equiv x_0^* = \pm 0.879077 \dots$

Superconductivity in the sub-critical temperature range ($T \lesssim T_c(\chi, x_0)$) is realized only if the free energy difference between the superconducting and the normal state is negative. Otherwise, the system is in the normal phase. According to formula (6), the free energy difference is positive if $\chi < \chi_s(x_0)$, with

$$\chi_s(x) = -\frac{3a}{\varphi(x)}, \tag{8}$$

and hence this inequality defines unstable regions, where superconductivity is suppressed. Examining Eq. (3) for $|x_0| \leq 0.288$, we find that for stable solutions (the values of $\mathcal{R}_t(\chi, x_0)$) to exist, the condition $\chi \geq \chi_m(x_0)$ must be satisfied. For $\chi = \chi_m(x_0)$, the values of $\mathcal{R}_t(x_0) \equiv \mathcal{R}_t(\chi_m(x_0), x_0)$ must be derived from the equation

$$\mathcal{R}_t = \mathcal{R}_1^* \exp \left[\frac{16x^2 \left[\tanh x \left(1 + \frac{\mathcal{R}_t^2}{16x^2} \right)^{3/2} - 1 \right]}{\mathcal{R}_t^2} - 1 \right],$$

and, thereafter, $\chi_m(x_0)$ is found as

$$\chi_m(x) = \ln \frac{\mathcal{R}_t(x)}{\mathcal{R}_1^*} \left[\frac{4}{\sqrt{16x^2 + \mathcal{R}_t^2(x)}} - \frac{\tanh x}{x} \right]^{-1}. \tag{9}$$

Note that both expressions: the one for $\mathcal{R}_t(x)$, as well as that for $\chi_m(x)$ are even functions of x . This estimate can be extended by the minimum value χ that is achieved for $\mathcal{R}_1 = 2$, when $-0.677 \leq x_0 \leq -0.288$ and $0.288 \leq x_0 \leq 0.677$. Then $\chi_m(x_0)$ is given by Eq. (9) with $\mathcal{R}_t(x_0) \equiv 2$. In particular, we have $\chi_m(0) = -0.579$, $\mathcal{R}_t(0) = 2.315$, $\chi_m(0.1) = -0.597$, $\mathcal{R}_t(0.1) = 2.281$, $\chi_m(0.2) = -0.654$, $\mathcal{R}_t(0.2) = 2.157$, $\chi_m(0.4) = -0.928$, $\mathcal{R}_t(0.4) = 2$, and $\chi_m(0.6) = -1.473$, $\mathcal{R}_t(0.6) = 2$. For $|x_0| > 0.677$ the minimum allowed value of χ is determined by $\chi_s(x_0)$, and then $\chi_m(x_0) \equiv \chi_s(x_0)$. The graph of χ_m as a function of x_0 is shown in Fig. 2.

The graphs of the ratio \mathcal{R}_1 vs χ for selected values of x_0 are shown in Fig. 1. Black dashed lines in the graphs indicate the horizontal asymptotes $\mathcal{R}_1 = \mathcal{R}_A(x_0)$, and unstable regions are cut off by the vertical red dashed lines $\chi = \chi_s$. Only the red line in the graphs defines stable solutions. However, for the graphs in Fig. 1(d–h) the solutions $\mathcal{R}_1 > \mathcal{R}_t$, and for the graphs in Fig. 1(j,k) the solutions $\mathcal{R}_1 > \mathcal{R}_t$ are unstable, and therefore superconductivity is suppressed. Hence, \mathcal{R}_t defines a stability threshold for these solutions. Details of the positions of all characteristic lines for graphs presented in Fig. 1 are given in Table 1.

Moreover, Fig. 1(i) refers to the case $\mathcal{R}_A(x_0) = \mathcal{R}_1^*$, for which x_0 has been derived by means of Eq. (7). For this case, no stable solution can exist at all. In our discussion, based on experimental data, we assume that $2 \leq \mathcal{R}_1 \leq 6$. However, the analysis can be extended beyond these limits.

In Table 2 the values of model parameters $|x_0|$, χ , \mathcal{R}_A , and χ_s for some superconducting materials are given. They have been found based on the experimental data (T_c , \mathcal{R}_1 , and \mathcal{R}_2) for a number of low-temperature superconducting materials. We also include the values of T_0 (the critical temperature) and $\nu_0 g$ (the dimensionless pairing parameter) determined within the standard BCS-model.

Note that the values of χ for Hg (α) and Pb are quite close to the boundary of unstable regions delineated by χ_s . Therefore, if $x_0 < 0$, then as we will discuss in the following Section 4, applying external pressure to the superconducting system turns it unstable and superconductivity is suppressed.

x_0	\mathcal{R}_A	χ_s	\mathcal{R}_t	Figure 1	x_0	\mathcal{R}_A	χ_s	\mathcal{R}_t	Figure 1
0	4	-1.279	—	(a)	± 0.87	3.537	-2.165	3.462	(h)
± 0.1	3.993	-1.289	—	(b)	± 0.8791	3.5278	-2.1856	3.5278	(i)
± 0.4	3.985	-1.447	—	(c)	± 0.9	3.507	-2.235	3.679	(j)
± 0.7	3.691	-1.827	2.173	(d)	± 1	3.404	-2.496	4.455	(k)
± 0.8	3.603	-2.013	2.943	(e)	± 1.3	3.062	-3.554	—	(l)
± 0.85	3.556	-2.120	3.316	(f)	± 1.5	2.818	-4.538	—	(m)
± 0.86	3.546	-2.142	3.389	(g)	± 2	2.206	-8.290	—	(n)

Table 1. Positions of horizontal asymptotes $\mathcal{R}_1 = \mathcal{R}_A$ and vertical cut-off lines $\chi = \chi_s$ for unstable regions in Fig. 1(a–n). Stability threshold values \mathcal{R}_t are also given.

SC material	T_c [K]	\mathcal{R}_1 [1]	\mathcal{R}_2 [1]	T_c^{\max} [K]	p_m [GPa]	$ x_0 $ [1]	χ [1]	\mathcal{R}_A [1]	χ_s [1]	Type	T_D [K]	T_0 [K]	$\nu_0 g$ [1]
Al	1.20	3.3	1.4	—	—	0.710	-1.138	3.683	-1.844	—	428	3.19	0.204
Cd	0.52	3.2	1.4	—	—	0.605	-0.943	3.766	-1.679	—	209	1.21	0.194
Hg (α)	4.15	4.6	2.4	—	—	1.175	-2.804	3.209	-3.058	—	71.9	29.8	1.135
In	3.4	3.6	1.7	—	—	0.528	0.483	3.820	-1.579	—	108	2.18	0.256
Nb ⁽⁰⁾	9.26	3.8	1.9	9.7	4.5	0.982	-2.073	3.423	-2.446	(D)	275	45.5	0.556
Nb ⁽¹⁾	9.26	3.6	1.87	9.95	10	0.600	0.689	3.770	-1.672	(A)	275	5.00	0.250
Nb ⁽²⁾	9.13	3.6	1.87	9.82	30	0.600	0.689	3.770	-1.672	(A)	275	4.93	0.249
Pb	7.19	4.3	2.7	—	—	1.092	-2.543	3.303	-2.773	—	105	46.1	1.215
Sn	3.72	3.5	1.6	5.3	11.3	0.866	-1.645	3.541	-2.155	(D)	200	14.0	0.377
Ta	4.41	3.6	1.6	4.5	40	0.436	0.345	3.876	-1.480	(A)	240	3.18	0.231
Tl	2.39	3.6	1.5	—	—	0.080	0.186	3.996	-1.285	—	78.5	1.98	0.272
V	5.38	3.4	1.5	16.5	120	0.807	-1.445	3.597	-2.028	(D)	380	16.6	0.320
Zn	0.855	3.2	1.6	—	—	0.714	-1.320	3.679	-1.851	—	237	2.66	0.223

Table 2. Experimental data $T_c = T_c(\chi, x_0, 0)$, $\mathcal{R}_1(\chi, x_0)$, $\mathcal{R}_2(\chi, x_0)$, $T_c^{\max} = T_c(\chi, x_0, p_m)$ and p_m of some superconducting (SC) materials. The corresponding values of $|x_0|$, χ , \mathcal{R}_A and χ_s , derived within the model are given, and the possible type of the T_c vs pressure dependence is indicated. Additionally, the values of $\nu_0 g$, and $T_0 = T_c(0, 0)$ derived for a given T_D (the Debye temperature) are included^{5,19,21,39,40}. The data for Nb⁽¹⁾ is taken from refs^{15,22}, and that for Nb⁽²⁾ from ref.⁴³.

Effects of External Hydrostatic Pressure

Response to external pressure: universal types of T_c vs pressure dependence. As we have shown in ref.²⁴ the inclusion of external pressure p in Eqs (1), (3–5) results in the variable x_0 being replaced by $x_0 \rightarrow \tilde{x}_0 = \tau(x_0 + \kappa p)$, where

$$\tau \equiv \tau(\chi, x_0, p) = \frac{T_c(\chi, x_0, 0)}{T_c(\chi, x_0, p)},$$

and $\kappa > 0$ is the coefficient of linear expansion in p . Then, from Eq. (1), we can find

$$T_c(\chi, x_0, p) = T_c(\chi, x_0, 0) \exp \left\{ \chi \left[\frac{\tanh[\tau(x_0 + \kappa p)]}{\tau(x_0 + \kappa p)} - \frac{\tanh x_0}{x_0} \right] \right\}. \quad (10)$$

In order to illustrate the discuss and predict the critical temperatures vs. pressure characteristics for superconducting systems under pressure, we will use Eq. (10), which after some algebra takes the form

$$t = \exp \left\{ \chi \left[\frac{t \tanh[t^{-1}(\alpha \mp 1)x_0]}{(\alpha \mp 1)x_0} - \frac{\tanh x_0}{x_0} \right] \right\},$$

where

$$t = \frac{T_c(\chi, x_0, p)}{T_c(\chi, x_0, 0)} \equiv \frac{T_c(p)}{T_c(0)}$$

and $\alpha = \kappa p / |x_0|$ is a dimensionless positive scaling parameter for pressure. The upper sign in “ \mp ” must be taken for the cases with $x_0 < 0$, whereas the lower one for $x_0 > 0$. Note that if $x_0 < 0$, there is a characteristic value of

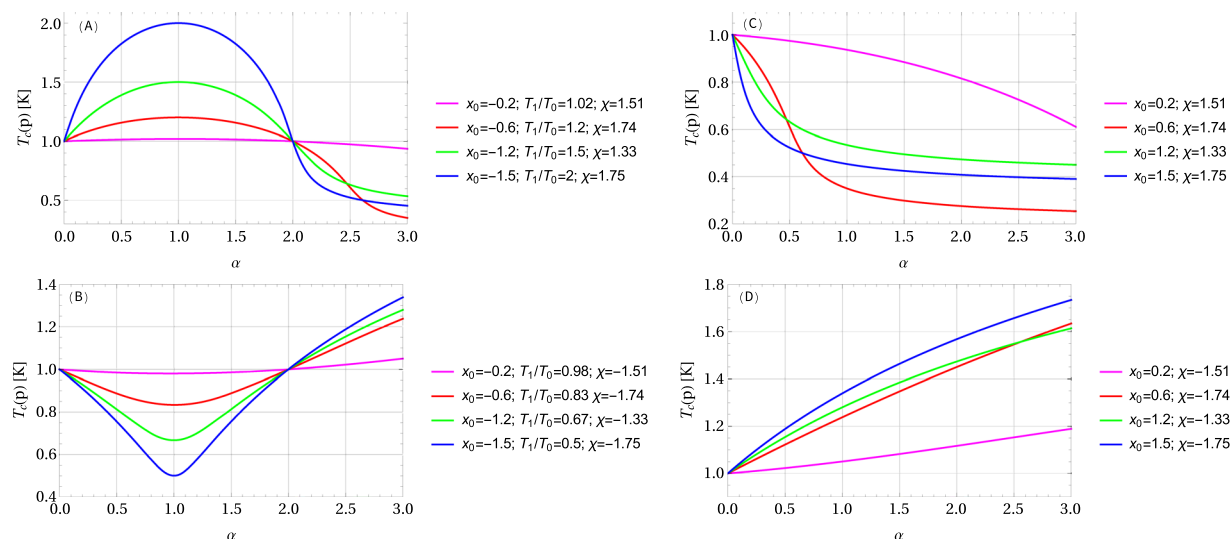


Figure 3. Four possible types of the dependence of the critical temperature on high external pressure. Here $\alpha = \kappa p/|x_0|$ is a dimensionless positive scaling parameter for pressure: **(A)** $T_c(1) > T_c(0)$ and $x_0 < 0$, then $\chi > 0$, **(B)** $T_c(1) < T_c(0)$ and $x_0 < 0$, then $\chi < 0$, **(C)** only $T_c(0)$ is given, $x_0 > 0$ and $\chi > 0$, **(D)** only $T_c(0)$ is given, $x_0 > 0$ and $\chi < 0$. It is shown that the shape of the curves changes, depending on the parameters x_0 and χ .

pressure $p_m = |x_0|/\kappa$, corresponding to $\alpha = 1$, for which the maximum or the minimum critical temperature is achieved.

The simple analytical model of the effect of high pressure on the critical temperature and other thermodynamic properties of superconductors presented in ref.³³, allowed us to identify four possible types of the dependence of the critical temperature T_c on high external pressure p . Namely, for $x_0 < 0$ the critical temperature $T_c(\chi, x_0, p)$ achieves a maximum for some $\chi > 0$, and a minimum for $\chi < 0$, if $p = -x_0/\kappa$. On the other hand, if $x_0 \geq 0$ the applied pressure drives the critical temperature downwards $T_c(\chi, x_0, p) \leq T_c(\chi, x_0, 0)$ if $\chi > 0$, or upwards $T_c(\chi, x_0, p) \geq T_c(\chi, x_0, 0)$ if $\chi < 0$. Consequently, for the four possible combinations of parameters $x_0 < 0$, $x_0 > 0$ and $\chi > 0$, $\chi < 0$, four different types of the response to the applied pressure are possible, as far as the critical temperature is concerned. These four cases are illustrated in Fig. 3. However, let us emphasize that Fig. 3 illustrates just several examples of possible examples of the response for some given values x_0 and χ , as the shape of the curves changes with different values of the critical temperature or with pressure scaling. In particular for the type-(A) and the type-(B) response, the dimensionless positive scaling parameter $\alpha = \kappa p/|x_0|$, and $\alpha = 1$ corresponds to the pressure giving the maximum or the minimum critical temperature, respectively.

For many superconducting systems, it is enough to take $0 \leq \alpha \leq 3$ and scale it with the appropriate values of pressure³³. On the other hand, for the type-(C) and the type-(D) behavior, the dimensionless positive scaling parameter α can be scaled at will if $x_0 > 0$, and it cannot be defined if $x_0 = 0$. Hence, for some cases $x_0 > 0$, it may occur that $\alpha = \kappa p/x_0$ runs into values of the order of 100. Examples of such materials are: NaCoO a type-(C) superconductor³⁴, with $T_c = 4.68$ K at $p = 0$, $T_c = 4.25$ K at $p = 1.5$ GPa modelled with $x_0 = 0.01$ and $\chi = 1$ for which $\mathcal{R}_1 = 3.760$ and $\mathcal{R}_2 = 0.939$, TlBaCuO being a type-(C) superconductor³⁵, with $T_c = 40$ K at $p = 0$, $T_c = 25$ K at $p = 1.76$ GPa, modelled with $x_0 = 1$ and $\chi = 1.6$ for which $\mathcal{R}_1 = 3.485$ and $\mathcal{R}_2 = 1.343$. NdFeAsOF a type-(C) superconductor³⁶, with $T_c = 45.4$ K at $p = 0$, $T_c = 25$ K at $p = 9.4$ GPa modelled with $x_0 = 0.84$ and $\chi = 1.68$ for which $\mathcal{R}_1 = 3.544$ and $\mathcal{R}_2 = 1.677$, and the vanadium which is of the type (D). Another example of a composed superconductor is YBaCuO — a type-(A) superconductor where a few different behaviors can be observed³⁷. Here we focus on two cases: $T_c = 17.1$ K at $p = 0$, $T_c = 23.8$ K at $p = 4.1$ GPa and $c_p = 2.1$ K/GPa with $x_0 = -1.585$, $\chi = 0.787$, for which $\mathcal{R}_1 = 3.456$ and $\mathcal{R}_2 = 1.971$, and $T_c = 17.1$ K at $p = 0$, $T_c = 45$ K at $p = 18$ GPa and $c_p = 20$ K/GPa with $x_0 = -1.629$, $\chi = 2.242$, for which $\mathcal{R}_1 = 3.356$ and $\mathcal{R}_2 = 3.009$, where based on a series of experimental data, we used the formulas given in ref.³³, Eqs (3) and (5).

Some other superconductors reveal their high pressure properties in the region of small α (of the order of 0.1 or 1). Examples of such systems include: niobium, zinc, tin, and SmBaCuO³⁸, where for the latter one $T_c = 78.5$ K at $p = 0$, $T_c = 86.3$ K at $p = 2$ GPa, $x_0 = 1$ and $\chi = -1.05$ for which $\mathcal{R}_1 = 3.595$ and $\mathcal{R}_2 = 0.978$. All of them are type-(D) materials. Another example of a low- α system is the type-(C) cadmium.

The experimental data and the corresponding values of the model parameters x_0 and χ for the superconducting elements that we have discussed above are given in Tables 2 and 3. Figures 4 and 5 show the graphs of the critical temperature as a function of pressure for some selected superconductors. For some composed novel superconducting systems, such as *e.g.* SmBaCuO, NaCoO, TlBaCuO, NdFeAsOF, being of the type-(C) or (D), additional experimental data for \mathcal{R}_1 , \mathcal{R}_2 , and c_p at $p = 0$ is not fully available, but we are still able to estimate the parameters x_0 and χ are from Eq. (9) for a few experimental points $(T_c(p), p)$, and then \mathcal{R}_1 and \mathcal{R}_2 can be determined from Eqs (3) and (5).

SC	T_c	\mathcal{R}_1	\mathcal{R}_2	c_p	$ x_0 $	χ	x_0	\mathcal{R}_A	χ_s	κ		$T_c^{\max/\min}$	p_m
material	[K]	[1]	[1]	[K/GPa]		[1]	[1]	[1]	[1]	[GPa ⁻¹]	Type	[K]	[GPa]
Hg (α)	4.156	4.6	2.4	-0.36	1.166	-2.787	-1.166	3.219	-3.025	0.196	(B)	1.83	59.6
Hg (β)	4.017	4.6	2.4	-0.44	1.166	-2.787	-1.166	3.219	-3.025	0.247	(B)	1.77	47.1
In	3.403	3.6	1.7	-0.436	0.546	0.521	0.546	3.808	-1.601	0.776	(C)		
Sn	3.732	3.5	1.6	-0.495	0.856	-1.334	-0.856	3.549	-2.135	0.253	(B)	2.20	33.9
Ta	4.301	3.6	1.6	-0.026	0.460	0.371	0.460	3.862	-1.504	0.0111	(C)		
Tl ⁽⁰⁾	2.380	3.6	1.5	0.24	0.170	0.200	-0.170	3.891	-1.309	4.549	(A)	2.385	0.0377
Tl ⁽¹⁾	2.380	3.603	1.535	0.11	0.280	0.247	-0.280	3.948	-1.360	1.018	(A)	2.395	0.275

Table 3. Experimental data T_c , \mathcal{R}_1 , \mathcal{R}_2 , and c_p for some superconducting materials. The value of model parameters $|x_0|$, χ , \mathcal{R}_A , χ_s , κ , $T_c^{\max/\min}$, and p_m are found within the presented model. The type of the T_c vs pressure dependence is determined based on their values. ref.¹⁹ provides the following values for Thallium: $T_c^{\max} = 2.395$ K and $p_m = 0.195$ GPa.

Characteristic ratios and pressure coefficient. The hydrostatic pressure applied to a superconducting system does not only affect its critical temperature, but also other thermodynamic characteristics, such as the characteristic ratios. Consequently, Eq. (3) must be replaced by

$$\mathcal{R}_1(\chi, x_0, p) = \mathcal{R}_1^* \exp \left\{ \chi \left[\frac{4}{\sqrt{[4\tau(x_0 + \kappa p)]^2 + \mathcal{R}_1^2(\chi, x_0, p)}} - \frac{\tanh[\tau(x_0 + \kappa p)]}{\tau(x_0 + \kappa p)} \right] \right\}.$$

Let us introduce yet another quantitative characteristics for a superconducting system subject to an external hydrostatic pressure: the pressure coefficient (at zero pressure) c_p . This quantity is currently well-researched for many superconducting materials¹. Within our model, as shown in ref.³³, the pressure coefficient at zero pressure is given by

$$c_p = \left. \frac{dT_c(\chi, x_0, p)}{dp} \right|_{p=0} = \frac{\chi \kappa T_c(\chi, x_0, 0) g(x_0)}{x_0 [1 + \chi g(x_0)]}, \quad (11)$$

where $g(x) = (x \cosh^{-2} x - \tanh x)/x$ is an even function of x , and $g(x) \leq 0$, $g(0) = 0$, $g(x) \rightarrow \infty$ for $|x| \rightarrow \infty$, and $g(\pm 1.639) = -0.4257$ is its minimum value. Note that, $c_p < 0$ if $x_0 < 0$ and $\chi < 0$, *i.e.* for the type-(B) behavior, and $c_p > 0$ if $x_0 > 0$ and $\chi < 0$, *i.e.* for the type-(D) behavior, which is correct since the critical temperature is then a decreasing or an increasing function of pressure, respectively. However, for the type-(A) and the type-(C) behavior, the sign of c_p may change, although the critical temperature is an increasing or a decreasing function of pressure, respectively. Therefore, an additional condition $1 + \chi g(x_0) > 0$ must be imposed on the parameters χ and x_0 resulting in the requirement that $\chi < -1/g(x_0)$. Note that $-1/g(x_0)$ has a minimum of 2.349 for $x_0 = \pm 1.639$, and it is proportional to $|x_0|$ if $|x_0| \rightarrow \infty$ and to $|x_0|^{-2}$ for $|x_0| \rightarrow 0$. Therefore, the condition $1 + \chi g(x_0) > 0$ does not impose any significant restrictions on the parameters χ and x_0 .

Pressure-induced emergence of superconductivity. There are many materials that undergo a superconducting phase transition under high pressure^{5,39,40}, with some examples listed in Tables 4 and 5. Please note that the experimental data originates from two different sources, and therefore, although both may list the same elements, there is some variation in the experimentally measured values.

We will now demonstrate how the developed model, with a single fluctuation of height of χ in the density of state, shifted a distance x_0 from the Fermi level, can be used to explain the effect of emergence of superconductivity in a system under external pressure. First of all, one should remember that the superconducting state is realized in the system if Eq. (3) has stable solutions $\mathcal{R}_1(\chi, x_0)$. However for a fixed x_0 , when $\chi < \chi_s$ in general, or rather $\chi < \chi_m$, superconductivity is suppressed in the system, as discussed in Section 3.3.

However, after applying an external pressure, the parameter x_0 is replaced by $\tilde{x}_0 = \tau(x_0 + \kappa p)$, as discussed at the beginning of the present section. Hence, when it reaches the value $\tilde{x}_0 > |x_0|$ such that $\chi_s(\tilde{x}_0) > \chi_s(x_0)$, superconductivity should appear.

Let us consider a few more specific examples, with some sets of parameters x_0 and χ characterizing a single fluctuation in the density of states.

- A Let $x_0 = 0$ and $\chi = -0.6$. Superconductivity is not realized in this system, because $\chi_m(0) = -0.579$ and $-0.6 < \chi_m(0)$. However, after applying an external pressure, x_0 is replaced by $\tilde{x}_0 = \tau \kappa p$, and when \tilde{x}_0 exceeds 0.1082 the superconducting state can be realized in the system for appropriate temperatures. This is because $-0.6 \geq \chi_m(0.1082)$ and $\mathcal{R}_1(-0.6, 0.1082) = 2.275$, and while $\tilde{x}_0 = \tau \kappa p = 0.4$, then $\mathcal{R}_1(-0.6, 0.4) = 3.1768$.
- B Let $x_0 = 0.2$ and $\chi = -0.67$. Superconductivity is suppressed in this system as well, because $\chi_m(0.2) = -0.654$. By placing the system under an external pressure, $\tilde{x}_0 = \tau(x_0 + \kappa p) = 0.4$ and superconductivity can be realized in the system at appropriate temperatures, because $\mathcal{R}_1(-0.67, 0.4) = 3.080$,

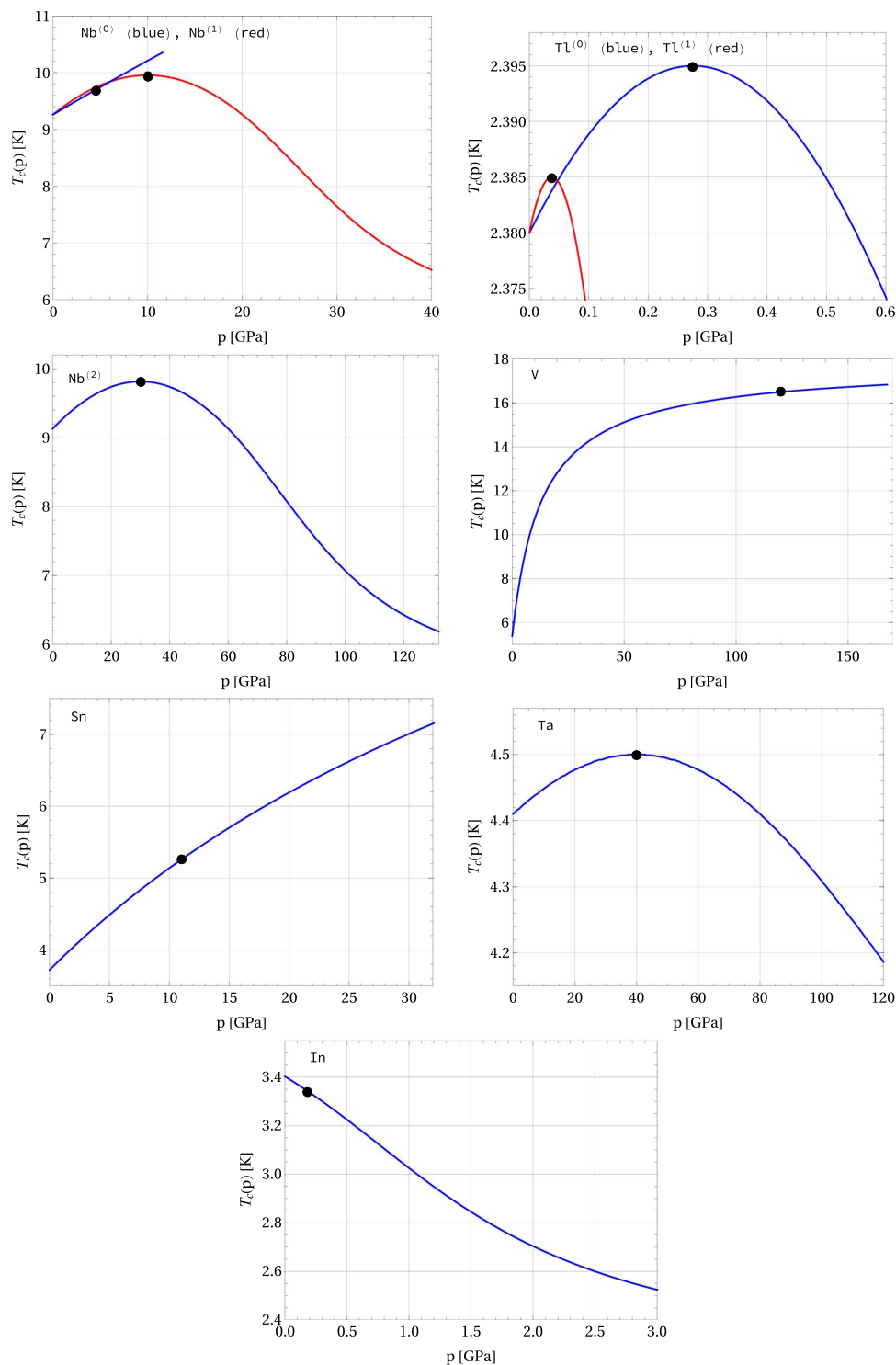


Figure 4. Critical temperature vs. pressure for selected superconductors: Nb⁽⁰⁾, Nb⁽¹⁾, Nb⁽²⁾, Tl⁽⁰⁾, Tl⁽¹⁾, V, Sn, Ta, and In. Black filled circles (●) indicate the experimental values listed in Table 2 for Nb⁽⁰⁾ (the critical temperature of 9.7 K at the pressure 4.5 GPa), Nb⁽¹⁾ (9.95 K at 10 GPa), and Nb⁽²⁾ (9.82 K at 30 GPa), V (16.5 K at 120 GPa), Sn (5.3 K at 11.3 GPa), and Ta (4.5 K at 40 GPa). The data for Tl⁽⁰⁾ (2.385 K at 0.0377 GPa) and Tl⁽¹⁾ (2.395 K at 0.275 GPa) is taken from Table 3, and the data for In (3.34 K at 0.18 GPa) is taken from ref.⁴².

while $\tilde{x}_0 = \tau(x_0 + \kappa p) = 0.7$ then $\mathcal{R}_1(-0.67, 0.7) = 3.437$.

- C If $x_0 = -0.2$ and $\chi = -0.67$, superconductivity appears in this system as in previous example, *i.e.* for $\tilde{x}_0 = \tau(x_0 + \kappa p) = 0.4$ or $\tilde{x}_0 = \tau(x_0 + \kappa p) = 0.7$. However, depending on the values of κ and τ , the threshold values of the pressure can differ significantly.

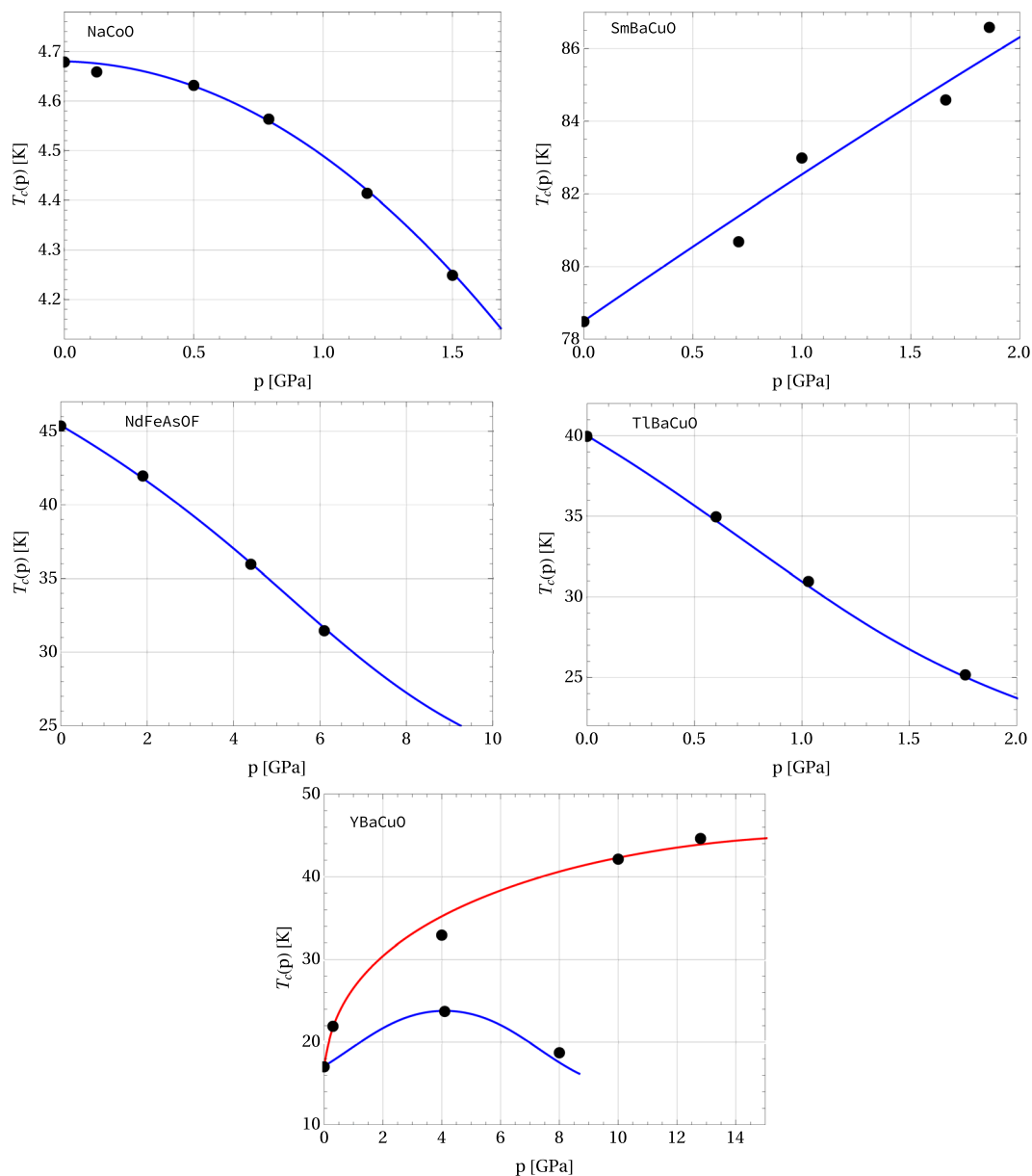


Figure 5. Critical temperature vs. pressure for selected superconductors: NaCoO, SmBaCuO, TlBaCuO, NdFeAsOF, YBaCuO. Black filled circles (●) indicate the experimental data according to refs^{34–38}, respectively.

Element	Li	B	O	Si	P	S	Ca	Sc	Fe	Ge	As
T_c [K]	20	11.2	0.6	8.5	18	17	15	0.34	2	5.4	2.7
p [GPa]	50	250	120	12	30	160	150	21	21	11.5	24
Element	Se	Br	Sr	Y	Sb	Te	I	Cs	Ba	Bi	Ce
T_c [K]	7	1.4	4	2.8	3.6	7.4	1.2	1.66	5	8.7	1.75
p [GPa]	13	150	50	15	8.5	35	25	8	20	9	5

Table 4. Elements undergoing a transition to the superconducting state under high pressure⁵.

D If the pressure increases, and $\tilde{x}_0 = \tau(x_0 + \kappa p)$ reaches values close to $x_0^* = \pm 0.879077 \dots$, solutions to Eq. (3) may fall into the instability region, and superconductivity is suppressed.

The phenomenon of pressure-induced superconductivity can be further illustrated with the example of the sulphur, using results presented in refs^{5,6}. The sulphur belongs to a class of materials, where superconductivity appears only under pressure. Finding the values of model parameters corresponding to the experimental data, we

Element	Li	B	O	Si	P	S	Ca	Sc	Fe	Ge	As	Se
T_c [K]	14	11	0.6	8.2	13	17.3	29	19.64	2.1	5.35	2.4	8
p [GPa]	30	250	100	15.2	30	190	217	106	21	11.5	32	150
Element	Br	Sr	Y	Sb	Te	I	Cs	Ba	Bi	Ce	Eu	Lu
T_c [K]	1.4	7	19.5	3.9	7.5	1.2	1.3	5	8.5	1.7	2.75	12.4
p [GPa]	100	50	115	25	35	25	12	18	9.1	5	142	174

Table 5. Elements undergoing a transition to the superconducting state under high pressure^{39,40}. The critical temperature for Li is estimated at 0.0004 K, so it should be left out of analysis here.

P	Case I			Case II		
	$T_c(p)$	\tilde{x}_0	χ_m	$T_c(p)$	\tilde{x}_0	χ_m
[GPa]	[K]	[1]	[1]	[K]	[1]	[1]
0	4.70	-0.1	-1.289	4.65	0.1	-1.289
100	13.4	0.940	-2.335	13.5	0.940	-2.335
160	17.0	1.206	-3.173	17.0	1.128	-2.893
250	21.0	1.542	-4.778	20.9	1.441	-4.221

Table 6. Parameters $\tilde{x}_0 = \tau(x_0 + \kappa p)$ and χ_m for sulphur under high pressure estimated based on refs^{5,6}. The two cases refer to (I) $x_0 = -0.1$, $\chi = -2.335$ and $\kappa = 0.0279 \text{ GPa}^{-1}$; (II) $x_0 = 0.1$, $\chi = -2.335$ and $\kappa = 0.0264 \text{ GPa}^{-1}$.

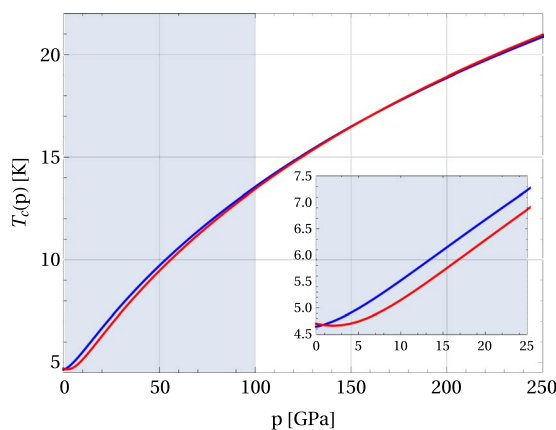


Figure 6. Two possible forms of superconductivity appearing in sulphur under pressure, corresponding to type-(B) (red curve) or type-(D) behavior (blue curve). The shaded area marks the unstable region, corresponding to the range of pressure where superconductivity is suppressed. The system becomes superconducting as soon as the pressure exceeds the threshold value beyond the shaded area⁶.

have $x_0 = \pm 0.1$ and $\chi = -2.335$. Consequently, since $\chi_m(\pm 0.1) = -0.597$ and $\chi < \chi_m(\pm 0.1)$, superconductivity does not appear. However, if the external pressure is applied and reaches the value of 100 GPa, the system becomes superconducting, which indicates that $\chi_m(\tilde{x}_0) = -2.335$. After estimating $T_c(p)$ for $p = 0, 100, 160$ and 250 GPa by fitting the numerical results presented in Fig. 6, one can find the value of κ from the relations

$$\chi_m(\tilde{x}_0) = -2.335 \text{ and } \tilde{x}_0 = \frac{T_c(0)}{T_c(100)}(\pm 0.1 + \kappa 100).$$

Using the values of the critical temperature given in Table 6, and calculating $\tilde{x}_0 = 0.940$ from Eq. (9), one finds $\kappa = 0.0279 \text{ GPa}^{-1}$ and $\kappa = 0.0264 \text{ GPa}^{-1}$ for the case $x_0 = -0.1$ and $x_0 = 0.1$, respectively.

The discussion shows that for systems where superconductivity is purely pressure-induced, the superconducting phase is not realized if the pressure is below a certain threshold value, since it is unstable there. In the particular case of the sulphur, assuming it to be a type-(B) or a type-(D) material leads to similar conclusions. And in both cases the critical temperature always increases with the pressure. Therefore, we should also expect that there are some materials with pressure-induced superconductivity, for which the critical temperature is a decreasing function of the pressure.

As a final remark to the present section, let us emphasize that one should keep in mind that a high pressure can change the structure of the material. These structural changes may imply a new form of the dispersion relation

and hence a different form of the fluctuation considered in this simple model. Consequently, the material can exhibit different properties.

Model Parameters and Experimental Data

Determination of model parameters from measurement data. Experimental data, such as the critical temperature T_c , the characteristic ratios \mathcal{R}_1 and \mathcal{R}_2 , as well as the pressure coefficient at zero pressure c_p , are widely available in the literature for various superconducting systems^{5,14–21}. However, as we have already mentioned before, the experimentally found values may vary by several percent as a result of differences in characterization techniques and methods.

Nevertheless, we still can use the experimental data to find the values of our model parameters: $|x_0|$ from Eq. (5), χ from Eq. (3), \mathcal{R}_A from Eq. (7), χ_s from Eq. (8) κ from Eq. (11). Note that a system with $c_p < 0$ and $\chi < 0$ must be of the type (B), and for $c_p > 0$ and $\chi > 0$ it must be of the type (A), hence $x_0 < 0$, and additional measurable parameters, *i.e.* the minimal or maximal critical temperatures $T_c^{\max/\min}$ at the pressure $p_m = -x_0/\kappa$ are given by

$$T_c^{\max/\min} = T_c \exp \left[\chi \left(1 - \frac{\tanh x_0}{x_0} \right) \right]. \quad (12)$$

The values of these parameters calculated for some superconducting elements are given in Table 3, with the data for T_c and c_p taken from ref.¹⁹.

Compatibility criterion for experimental data. The developed model allows us to establish a very useful criterion for testing compatibility of experimental data. The criterion verifies whether the estimated values of \mathcal{R}_1 and \mathcal{R}_2 are compatible with the data for T_c and $T_c^{\max/\min}$ for type-(A) or type-(B) superconductors.

The criterion is established as follows: For a superconducting system, the values of \mathcal{R}_1 and \mathcal{R}_2 found experimentally allow us to derive the parameter x_0 from Eq. (5), and then by substituting \mathcal{R}_1 and x_0 into Eq. (3), we can find the corresponding value of the parameter χ . On the other hand, for the same superconductor (either type-(A) or type-(B)) after substituting their critical temperatures T_c and $T_c^{\max/\min}$ into Eq. (12), the parameter χ can be calculated again using an alternative method. These both values of the parameter χ estimated from the experimental data should be identical. Therefore, by comparing them we can directly evaluate the precision of experimental measurements.

Referring to the experimental data for superconducting materials discussed in this paper as examples, it is worth to notice that the values of χ obtained for the tantalum are equal to 0.345, as given in Table 2, and 0.344 when it is found from Eq. (12). The two values of χ obtained for the thallium are equal to 0.200 or 0.247 for $\text{TI}^{(0)}$ and $\text{TI}^{(1)}$ (Table 3), and 0.660 or 0.248 when it is found from Eq. (12). Finally, the values of the same parameter found for the niobium are equal to 0.689 (Table 2) for $\text{Nb}^{(1)}$, and 0.689 as well, if found from Eq. (12).

A brief comparison of the values of χ for the thallium, given in Table 3, immediately indicates that the estimates of parameters presented in ref.¹⁹ as $\text{TI}^{(0)}$ are not correct, whereas those given as $\text{TI}^{(1)}$ pass the compatibility test. Moreover, the experimental data for the niobium presented in Table 2, *i.e.* $\text{Nb}^{(0)}$, $\text{Nb}^{(1)}$, $\text{Nb}^{(2)}$, are not compatible, and one should definitely reject the claim that it is a type-(D) material.

With the example of the thallium it has been shown that a simple estimate of the experimental data given in ref.¹⁹, that is the line $\text{TI}^{(0)}$ is in contradiction with other parameters of the model. However, if the experimental data were slightly different, but still within the accuracy of the measurements, and the values of c_p and p_m were estimated again, the received results shown as the line $\text{TI}^{(1)}$ would coincide quite well with the points showing the experimental data. Therefore, the postulated values of $c_p = 0.24$ K/GPa and $p_m = 0.195$ GPa¹⁹ should rather be replaced by $c_p = 0.11$ K/GPa and $p_m = 0.275$ GPa.

A careful analysis of the examples of $\text{TI}^{(0)}$ and $\text{TI}^{(1)}$ points to the fact that the simple model is sensitive to minor changes in the output parameters. At the same time, it imposes some conditions on the postulated parameters, such as on the values of c_p and p_m , so that the results can match the experimental data in the best possible way.

Conclusions

In our previous work³³, we have identified and discussed four universal types of the response of superconducting systems to an external high pressure, in terms of the dependence of the critical temperature on pressure. In the present paper, within that model³³, we have discussed further pressure-related properties of some specific superconducting materials and referred them to available experimental data. The wide range of numerical results indicates that experimental data can be successfully used to find the critical temperature as a function of pressure, and discuss other properties of superconducting systems under high pressure. It should be emphasized that the presented approach contains a significantly simplified density of states, therefore it can be applied to complex superconductors only to a limited extent. Nevertheless, the available experimental data support the observation that the dependence of the critical temperature on external pressure can be identified as being one of four general types: (A), (B), (C), or (D).

Worth noting is that the results obtained within our model are sensitive to the uncertainty of experimental data, which is often not analyzed in papers presenting experimental results. Therefore, even for the same superconducting system and the same parameter, experimental results obtained using different measurement techniques, provide values that may sometimes differ to a relatively large extent. This dispersion in the experimental data can lead to contradictory conclusions, as *e.g.* for the niobium.

For the same reason, we did not identify the type of some superconductors given in Table 2. For instance, in the case of the aluminium, using the compatibility criterion formulated in the paper, we have found the data given in the literature^{20,39,40} to be incompatible, although according to refs.^{5,41} the aluminium should be of a type-(C)

system. We also doubt that the transition temperature estimated for Lithium is $T_c = 0.0004 \text{ K}^{39,40}$, since the critical temperature should be enhanced by ca. 3.5×10^4 times. Hence, the proposed scenario of superconductivity appearing under pressure seems to be more convincing.

As a final remark, let us emphasize that the presented simplified model is based on the assumption that the crystal structure of a superconductor is stable under high pressure. In general, however, high pressure can induce structural phase transitions in some materials, and properties of such systems may change drastically. Consequently, the one-particle dispersion relation ξ_k assumes a new, stable form, and if the superconductivity is not suppressed, the new system can be analyzed again within the conformal transformation method. However, compared to the original system, before the structural phase transition has taken place, the system with a new structure may reveal quite different properties. In particular, one type of the dependence of the critical temperature on pressure might be replaced by another, when the pressure is being increased. Therefore, one can expect that in quasi-two-dimensional systems, such as films of elements discussed in ref.⁵, superconductivity appears due to an essential change in the one-particle dispersion relation ξ_k . Such systems can be considered within the developed model as well^{13,24,33}.

Data Availability

All data generated or analyzed during this study are included in this published article.

References

- Ohmura, A. *et al.* Pressure effect on critical temperature for superconductivity and lattice parameters of AlB_2 -type ternary silicide $\text{YbGa}_{1.1}\text{Si}_{0.9}$. *Phys. Rev. B* **84**, 104520 (2011).
- Fu, Y. *et al.* High-pressure phase stability and superconductivity of pnictogen hydrides and chemical trends for compressed hydrides. *Chem. Mater.* **28**, 17461755 (2016).
- Selvamani, P., Vaitheeswaran, G., Kanchana, V. & Rajagopalan, M. Effect of pressure on the superconducting transition temperature of Nb–Zr and Ti–V. *Physica C* **370**, 108112 (2002).
- Gu, Q., Lu, P., Xia, K., Sun, J. & Xing, D. High-temperature superconducting phase of HBr under pressure predicted by first-principles calculations. *Phys. Rev. B* **96**, 064517 (2017).
- Buzza, C. & Robbie, K. Assembling the puzzle of superconducting elements: A Review. *Supercond. Sci. Technol.* **18**, R1–R8 (2005).
- Drozdov, A. P., Eremets, M. I., Troyan, I. A., Ksenofontov, V. & Shylin, S. I. Conventional superconductivity at 203 kelvin at high pressures in the sulfur hydride system. *Nature* **525**, 73 (2015).
- Durajski, A. P. Quantitative analysis of nonadiabatic effects in dense H_2S and PH_3 superconductors. *Scientific Reports* **6**, 38570 (2016).
- Ge, Y., Zhang, F. & Yao, Y. First-principles demonstration of superconductivity at 280 K in hydrogen sulfide with low phosphorus substitution. *Phys. Rev. B* **93**, 224513 (2016).
- Grechnev, G. E. *et al.* Interplay between lattice and spin states degree of freedom in the FeSe superconductor: Dynamic spin state instabilities. *J. Phys.: Condens. Matter* **25**, 046004 (2013).
- Papaconstantopoulos, D. A., Klein, B. M., Mehl, M. J. & Pickett, W. E. Cubic H_2S around 200 GPa: An atomic hydrogen superconductor stabilized by sulfur. *Phys. Rev. B* **91**, 184511 (2015).
- Duan, D. *et al.* Pressure-induced metallization of dense $(\text{H}_2\text{S})_2\text{H}_2$ with high- T_c superconductivity. *Scientific Reports* **4**, 6968 (2014).
- Mulak, M. & Gonczarek, R. Discontinuous phase transitions in S-paired Fermi systems. *Acta Physica Polonica-Series A: General Physics* **92**, 1177 (1997).
- Krzyzosiak, M., Gonczarek, R., Gonczarek, A. & Jacak, L. Applications of the conformal transformation method in studies of composed superconducting systems. *Frontiers of Physics* **11**, 117407 (2016).
- Fetter, A. L. & Walecka, J. D. *Quantum Theory of Many-Particle Systems*, McGraw-Hill Book Company (1971).
- Ashcroft, N. W. & Mermin, N. D. *Solid State Physics*, Holt, Rinehart and Winston, ch. 34 *Superconductivity* (1976).
- Kittel, C. *Introduction to Solid State Physics*, John Wiley and Sons, Inc. NY, ch. 11 (1966).
- Spalek, J. *Introduction to Condensed Matter Physics*, Wydawnictwo Naukowe PWN SA, Warsaw, ch. 17 (2015).
- Ibach, H. & Lüth, H. *Solid State Physics. An Introduction to Principles of Material Science*, Springer-Verlag Barlin Heidelberg, ch. 10. 5 (1995).
- Jennings, L. D. & Swenson, C. A. Effects of Pressure on the Superconducting Transition Temperatures of Sn, In, Ta, Tl and Hg. *Phys. Rev.* **112**, 31 (1958).
- Coulthard, M. A. Effects of pressure on superconducting properties of simple metals. *J. Phys. F: Met. Phys.* **1**, 195 (1971).
- Powell, R. W. & Touloukian, Y. S. Thermal Conductivities of the Elements. *Science* **181**, 999 (1973).
- Meservey, R. & Schwartz, B. B. *Equilibrium properties: Comparison of experimental results with predictions of the BCS theory* In: *Superconductivity, volume 1*, Editor: R. D. Parks, Marcell Dekker, Inc., New York, 1969, ch. 2.
- Shrivastava, S. K. Search for higher critical temperature (T_c) in superconducting materials. *International Journal of Engineering & Scientific Research (IJESR)* **5**, 40 (2017).
- Gonczarek, R., Krzyzosiak, M., Gonczarek, A. & Jacak, L. Analytical assessment of some characteristic ratios for s-wave superconductors. *Frontiers of Physics* **13**, 137403 (2018).
- Gonczarek, R., Krzyzosiak, M., Jacak, L. & Gonczarek, A. Coexistence of spin-singlet s- and d-wave and spin-triplet p-wave order parameters in anisotropic superconductors. *phys. stat. sol. (b)* **244**, 3559 (2007).
- Gonczarek, R., Krzyzosiak, M., Gonczarek, A. & Jacak, L. *Conformal Transformation Method in Studies of High- T_c Superconductors — Beyond the Van Hove Scenario* In: *Superconductivity and Superconducting Wires*, Editors: Matteri, D., Futino, L. Nova Science Publishers, Hauppauge, New York, 2010, ch. 5. 3296 (2008).
- Gonczarek, R., Jacak, L., Krzyzosiak, M. & Gonczarek, A. Competition mechanism between singlet and triplet superconductivity in the tight-binding model with anisotropic attractive potential. *Eur. Phys. J. B* **49**, 171 (2006).
- Gonczarek, R., Gładysiewicz, M. & Mulak, M. On Possible Formalism of Anisotropic Fermi Liquid and BCS-type Superconductivity. *Int. J. Mod. Phys. B* **15**, 491 (2001).
- Gonczarek, R., Krzyzosiak, M. & Mulak, M. Valuation of characteristic ratios for high- T_c superconductors with anisotropic gap in the conformal transformation method. *J. Phys. A* **37**, 4899 (2004).
- Gonczarek, R., Gładysiewicz, M. & Mulak, M. Equilibrium states and thermodynamical properties of d-wave paired HTSC in the tight-binding model. *phys. stat. sol. (b)* **233**, 351 (2002).
- Gonczarek, R. & Mulak, M. Enhancement of critical temperature of superconductors implied by the local fluctuation of EDOS. *Phys. Lett. A* **251**, 262 (1999).
- Gonczarek, R., Krzyzosiak, M. & Gonczarek, A. Islands of stability of the d-wave order parameter in s-wave anisotropic superconductors. *Eur. Phys. J. B* **61**, 299 (2008).

33. Krzyzosiak, M., Gonczarek, R., Gonczarek, A. & Jacak, L. Simple analytical model of the effect of high pressure on the critical temperature and other thermodynamic properties of superconductors. *Scientific Reports* **8**, 7709 (2018).
34. Lorenz, B., Cmaidalka, J., Meng, R. L. & Chu, C. W. Effect of hydrostatic pressure on the superconductivity in $\text{Na}_x\text{CoO}_2 \cdot y\text{H}_2\text{O}$. *Phys. Rev. B* **68**, 132504 (2003).
35. Looney, C., Schilling, J. S., Doyle, S. & Hermann, A. M. Possibility for oxygen relaxation below 15 K in superconducting $\text{Ti}_2\text{Ba}_2\text{CuO}_{6+x}$ instabilities. *Physica C* **289**, 203210 (1997).
36. Abdel-Hafiez, M. *et al.* High-pressure phase diagram of $\text{NdFeAsO}_{0.9}\text{F}_{0.1}$: Disappearance of superconductivity on the verge of ferromagnetism from Nd moments. *Phys. Rev. B* **98**, 094504 (2018).
37. Sadewasser, S., Schilling, J. S., Paulikas, A. P. & Veal, B. M. Pressure dependence of T_c to 17 GPa with and without relaxation effects in superconducting $\text{YBa}_2\text{Cu}_3\text{O}_x$. *Phys. Rev. B* **61**, 741–749 (2000).
38. Marcus, J. *et al.* High temperature superconductivity in $\text{SmBa}_2\text{Cu}_3\text{O}_{7-x}$: transport properties and effect of pressure. *J. Phys. France* **49**, 111 (1988).
39. Debessai, M., Hamlin, J. J. & Schilling, J. S. Comparison of the pressure dependences of T_c in the trivalent d-electron superconductors Sc, Y, La, and Lu up to megabar pressures. *Phys. Rev. B* **78**, 064519 (2008).
40. Debessai, M. *et al.* Pressure-induced superconductivity in europium metal. *J. Phys.: Conf. Series* **215**, 012034 (2010).
41. Gubser, D. U. & Webb, A. W. High-pressure effects on the superconducting transition temperature of aluminium. *Phys. Rev. Lett.* **35**, 104–107 (1975).
42. Kan, L. S., Lazarev, G. B. & Makarov, V. I. On the superconductivity of tin and iridium under pressure. *Soviet Physics JEPT* **13**, 317–319 (1961).
43. Struzhkin, V. V., Timofeev, Y. A., Hemley, R. J. & Mao, H. K. Superconducting T_c and electron-phonon coupling in Nb to 132 GPa: magnetic susceptibility at megabar pressures. *Phys. Rev. Lett.* **79**, 4262 (1997).

Acknowledgements

This research is supported by Ministry of Science and Higher Education (Poland) in 2018–2020.

Author Contributions

M.K. and R.G. wrote the main manuscript text, M.K. and A.G. prepared Figures 1–6, R.G. and L.J. performed analytical calculations. All authors reviewed the manuscript.

Additional Information

Competing Interests: The authors declare no competing interests.

Publisher's note: Springer Nature remains neutral with regard to jurisdictional claims in published maps and institutional affiliations.



Open Access This article is licensed under a Creative Commons Attribution 4.0 International License, which permits use, sharing, adaptation, distribution and reproduction in any medium or format, as long as you give appropriate credit to the original author(s) and the source, provide a link to the Creative Commons license, and indicate if changes were made. The images or other third party material in this article are included in the article's Creative Commons license, unless indicated otherwise in a credit line to the material. If material is not included in the article's Creative Commons license and your intended use is not permitted by statutory regulation or exceeds the permitted use, you will need to obtain permission directly from the copyright holder. To view a copy of this license, visit <http://creativecommons.org/licenses/by/4.0/>.

© The Author(s) 2019